H_∞ Formation Control and Obstacle Avoidance for Hybrid Multi-agent Systems

Dong Xue, Jing Yao and Jun Wang

***Abstract*—In this paper, a new concept of H_∞ formation is proposed to handle a group of agents navigating in a free and an obstacle-laden environment while maintaining a desired formation and changing formations when required. With respect to the requirements of changing formation subject to internal or external events, a hybrid multi-agent system (HMAS) is formulated in this paper. Based on the fact that obstacles impose the negative effect on the formation of HMAS, the H_∞ formation is introduced to reflect the above disturbed situation and quantify the attenuation level of obstacle avoidance via the H_∞-norm of formation stability. An improved Newtonian potential function and a set of repulsive functions are employed to guarantee the HMAS formation-keeping and collision-avoiding from obstacles in a path planning problem, respectively. Simulation results in this paper show that the proposed formation algorithms can effectively allow the multi-agent system to avoid penetration into obstacles while accomplishing prespecified global objective successfully.**

***Index Terms*—H_∞ formation; obstacle avoidance; artificial potential field; hybrid multi-agent system**

I. Introduction

In recent years, there has been a spurt of interest in the area of cooperative control for multiple agents due to its challenging features and many applications, e.g., formation control [1], [2], obstacles avoidance [3], [4], rendezvous [5], flocking [6], foraging [7], troop hunting, and payload transport. Referring to the existing literature, it is obvious that multiple agents can perform tasks faster and more efficiently than a single one. The existing approaches for cooperative control of MASs fall into several categories, including behavior-based, artificial potential, virtual structure, leader-follower, graph theory and decentralized control methods. Other methods and research aspects of the cooperative control for MASs can be found in [8]–[10].

As one key branch of cooperative control, formation and obstacle avoidance problems of multi-agent systems have been received significant attentions [1]–[4], [8], [11]. In this case, the MAS is usually required to follow a trajectory while maintaining a desired formation and avoiding obstacles. In some practical situations, the group of agents may be necessary to perform certain maneuvers, such as split, reunion and reconfiguration, in order to negotiate the obstacles [2], [12]. Although the formation problem for MASs is attracting increasingly research attention, there are still several open fields deserving further investigation, such as robustness, fragility, and effectiveness of formation. With respect to most robustness analysis of MASs, such as [13]–[15], the agents are investigated under uncertain environments with external disturbances. However, in some sense, obstacles in the navigational path can also be regarded as a disturbance from environment, which would impair the performance of formation stability. Furthermore, the influence of obstacles is usually negligible when the distances between agents and obstacles exceed certain range threshold. Inspired by obstacle avoidance issue and H_∞ control theory, we introduce a new concept of H_∞ formation, which treats the effects of obstacles as certain exterior disturbances, to handle the formation problem of MASs in clustered environment. Then a Lyapunov approach is employed to deal with H_∞ analysis.

Artificial potential field (APF) method is widely used in coordination control of MASs due to its simplicity and efficiency [7], [16], which was first introduced by [17] for formation and obstacle avoidance of MASs. Since then, several literatures have attempted to improve the performance of APF method. In [18], bifurcation theory is used to reconfigure the formation through a simple free parameter change to reduce the computational expense. By introducing a new concept of artificial potential trenches in [11], the scalability and flexibility of robot formations are improved. The basic idea of potential field theory is to create a workshop where the agents are counterbalanced with each other by the interactive potential force between them, and suffered a repulsive force from obstacles to steer around them [19]. Despite all the advantages of APFs, the lack of accurate representations of obstacles with arbitrary shapes is regarded as one major limitation to generally extend to practical applications. A potential function based on generalized sigmoid functions which can be generated from the combinations of implicit primitives or from sampled surface data, is proposed in [20]. Using the optical flow, [21] have achieved the automatic detection of obstacles in virtual environment. The formation control with obstacle avoidance is highly related to the flocking problems in [6], where only the obstacles with simple shapes are taken into account. In this paper, we assume the boundary functions of arbitrary obstacles can be known from the implicit functions which can be constructed from sensor readings or image data. By combining the artificial potential model and the negotiating results with obstacles, a resultant artificial repulsive force is developed to guarantee the obstacles avoidance.

In addition, it may happen that the MASs are desired

D. Xue is with the Institute for Information-oriented Control, Technische Universität München, D-80290 München, Germany; dong.xue@tum.de.

Jing Yao and Jun Wang are with the Department of Control Science and Engineering, Tongji University, Shanghai, P. R. China. e-mail: yaojing@tongji.edu.cn, junwang@tongji.edu.cn.

Jing Yao is also with the Department of Electronic and Computer Engineering, The Hong Kong University of Science and Technology, Hong Kong SAR, P. R. China.

to perform various formation shapes to achieve specified navigational objective. As a result, it is necessary for a MAS to possess the ability of changing formation shape during the navigation, such as split, rejoin and reconfiguration. In this case, the MASs consist of both continuous variables and discrete events. In [2], a triple (group element $\mathfrak{g}$, shape variable $\mathfrak{r}$, control graph $\mathfrak{H}$) is employed to model the mobile robots and meet the requirement of changing formations. Furthermore, a Petri-potential-fuzzy hybrid controller is presented for the motion planning of multiple mobile robots with multiple targets in a clustered environment in [22]. In this paper, a hybrid formation controller is proposed where the formation changes as events (tasks) occur. In practice, the correspondence between tasks and formation can be prespecified at the initialization step, as well as be created intelligently by the embedded processors in each agent during the implementation. It is remarkable that the hybrid multi-agent systems exhibit continuous-state dynamics and discrete behavior jumping between formations. Then we formulate the HMAS by a hybrid machine owing to its advantages of illustrating inputs and outputs explicitly [23], [24].

The paper proceeds as follows. The formation control and obstacle avoidance problem are addressed in Section II. In Section III, a new concept of H_∞ formation and technical proofs are provided. In Section IV, we discuss the obstacle-avoidance functions. Simulation results to illustrate the results are presented in Section V. Conclusions and future work are provided in Section VI.

Notation I.1. *Throughout the paper, let* $\overline{\mathbb{Z}}$ *be the set of positive integers and* $\mathbb{J} = [t_0, +\infty)\,(t_0 \geq 0)$. $\mathbb{R}^n$ *represents the real Euclidean* n*-dimensional vector space. For* $x = (x_1, \ldots, x_n)^\top \in \mathbb{R}^n$, *the norm of* x *is* $\|x\| \triangleq \left(x^\top x\right)^{\frac{1}{2}}$, *where the symbol* $(\cdot)^\top$ *denotes the transpose of a matrix or a vector.* I_n *denotes the identity matrix of order* n *(for simplicity* I *if no confusion arises).* $\mathfrak{L}_2[0,\infty)$ *is the Lebesgue space of* R^n*-valued vector-functions* $g(\cdot)$, *defined on the time interval* $[0,\infty)$, *with the norm* $\|g\|_2 \triangleq \left(\int_0^\infty \|g(t)\|^2\right)^{\frac{1}{2}} dt$.

II. Problem formulation and preliminaries

Consider a multi-agent system with N nodes and an undirected graph topology $\mathfrak{G} = (\nu, \varepsilon)$; ν and ε are the set of vertices and the set of edges (i.e, $\varepsilon \in \nu \times \nu$), respectively. The notation (i,j) or (j,i) equivalently denotes the edge of the graph between node i and node j. Furthermore, a graph is connected if there exists a path between every pair of distinct nodes, otherwise it is disconnected.

Before proceeding further, the following assumptions are made in this paper.

1) Each agent is equipped with sensors and computational hardware that allow it to detect the distances to the obstacles within the sensing range. Furthermore, the agent can access its position in the world coordinate system and broadcast to its neighboring agents. The wireless communication has a limited range and is assumed to be imperfect, i.e., links may be broken.

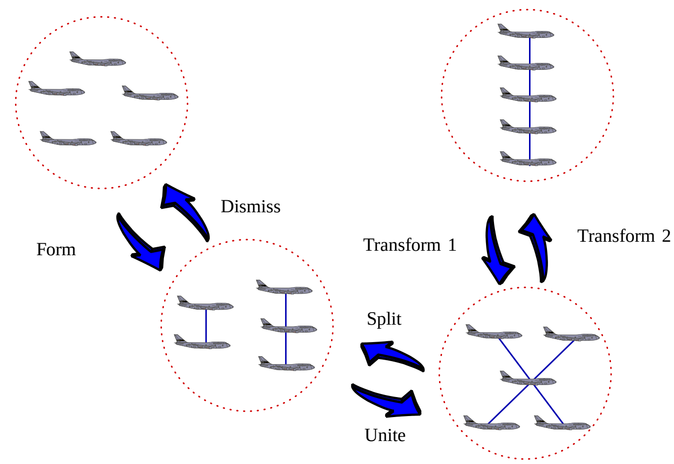

Fig. 1. Example of a hybrid multi-agent system performing under different events

2) The multi-agent system has a task set Σ and a formation set $\mathbb{F}$ which meet actual project needs before initiation. And suppose all agents know the information of Σ and $\mathbb{F}$, as well as the desired formation shape and trajectories in every step.

Referred to hybrid machine presented in [23], [24] and associated with the practical application, we consider a special class of hybrid multi-agent system (HMAS) which is modeled by an elementary hybrid machine (EHM) [25] as:

$$\mathrm{HMAS} = \left(Q, \Sigma, Dy, E, (\Delta^0, x(0))\right). \tag{1}$$

The elements of HMAS are denoted as follows. $Q = \{q_0, q_1, \ldots, q_{m-1}\}$ is a set of vertices (discrete states); in formation control, each discrete state $q_i \in Q$ corresponds to a desired formation shape Δ^i, and we denote a set of formation shape as $\mathbb{F} := \{\Delta^0, \Delta^1, \ldots, \Delta^{m-1}\}$. $\Sigma = \{\mathcal{H}_{q_i q_j}, q_i, q_j \in Q\}$ $(i,j = 0, \ldots, m-1)$ is a finite (task) set of event labels; $(q_0, x(0))$ is the initial desired formation and state of HMAS, respectively. $E = \{\left(q_i, \mathcal{H}_{q_i q_j}, q_j, x^0_{q_0}\right) : q_i, q_j \in Q\}$ is a set of edges (transition-paths), where q_i is exited vertex and q_j is entered one. If the event $\mathcal{H}_{q_i q_j}$ is triggered, consequently the formation of HMAS transits from Δ^i to Δ^j. For example, Fig. 1 shows a sequence of admissible collective behaviors of a HMAS triggered by event set $\Sigma = \{\text{form, dismiss, split, unite, transform 1, transform 2}\}$.

Remark II.1. *In practical application, the multi-agent system is always assigned multiple tasks in the navigation and each task may correspond to multiple formation shapes. Similarly to the deterministic automaton described in [26], we suppose the HMAS is deterministic, namely, there cannot be two transitions with the same event label. It is worth mentioning that the following theoretical analysis is available for nondeterministic HMAS, i.e., there can be multiple transitions triggered by the same event.*

Dy is the dynamics of HMAS and for each agent i and $q \in Q$, which is described by

$$\dot{x}_i(t) = f(t,x) + \sum_{j=1}^{N} J_{ij}(t) x_j(t) + u_i^q(t) + C_i w_i(t), \tag{2}$$

where $i \in \{1,2,\ldots,N\}$, $t \in \mathbb{J}$, $x_i(t) \in \mathbb{R}^{n\times 1}$, $x=[x_1^\top,x_2^\top,\ldots,x_N^\top]^\top$, C_i are real constant matrices with appropriate dimensions. $f(t,x) : \mathbb{J}\times\mathbb{R}^{N\times n} \to \mathbb{R}^{n\times 1}$ is continuously differentiable, representing the group motion (i.e. path of the HMAS). $J(t)=(J_{ij}(t))_{N\times N}$ is the time-varying coupling configuration matrix representing the communication strength and communicational topology of the HMAS. If there is an interconnection between agent i and agent $j(j\neq i)$, then $J_{ij}(t)=J_{ji}(t)>0$; otherwise, $J_{ij}(t)=J_{ji}(t)=0$ and the diagonal elements of matrix $J(t)$ are defined by

$$J_{ii}(t)=-\sum_{j=1,j\neq i}^{N}J_{ij}(t)=-\sum_{j=1,j\neq i}^{N}J_{ji}(t). \tag{3}$$

$w_i(t)$ here denotes the obstacle-avoiding function, which will be derived from potential function in Section VI.

Moreover, the formation controller in this paper is derived by extending the one in [1] into multi-formation case ($q\in Q$):

$$\begin{aligned}u_i^q(t)=&\sum_{\substack{j=1\\ j\neq i}}^{N}2\left(x_j(t)-x_i(t)-\Delta_{ij}^q\right)\\&\left[\frac{S_a}{L_a^2}e^{-\frac{\|x_j(t)-x_i(t)-\Delta_{ij}^q\|^2}{L_a^2}}-\frac{S_r}{L_r^2}e^{-\frac{\|x_j(t)-x_i(t)-\Delta_{ij}^q\|^2}{L_r^2}}\right.\\&\left.+S_r\left(\frac{1}{L_r^2}+\frac{1}{L_a^2}\right)e^{-(\frac{1}{L_r^2}+\frac{1}{L_a^2})\|x_j(t)-x_i(t)-\Delta_{ij}^q\|^2}\right],\end{aligned} \tag{4}$$

where $\Delta_{ij}^q\in\mathbb{R}^{n\times 1}$ and $\Delta^q=\left(\Delta_{ij}^q\right)_{N\times N}\in\mathbb{F}$ is the formation-shape matrix of the multi-agent system with $\Delta_{ij}^q=-\Delta_{ji}^q$ and $\Delta_{ii}^q=0$. Parameters S_a, S_r, L_a, and L_r are positive constants representing the strengths and effect ranges of the attractive and repulsive forces, respectively; and with the constraint:

$$\begin{aligned}\frac{S_a}{S_r}>&\frac{L_a^2}{L_r^2}e^{-(\frac{1}{L_r^2}-\frac{1}{L_a^2})\|x_j(t)-x_i(t)-\Delta_{ij}^q\|^2}\\&-\left(1+\frac{L_a^2}{L_r^2}\right)e^{-\frac{\|x_j(t)-x_i(t)-\Delta_{ij}^q\|^2}{L_r^2}},\end{aligned} \tag{5}$$

where $L_a>L_r$.

Remark II.2. *Compared to the formation controller given in [1], the formation controller in this paper is designed to achieve more complicated control objects, such as formation switching in clustered environment. Furthermore, it is worth mentioning that the obstacle-avoiding function $w_i(t)$ ($i=1,\ldots,N$) as a part of the controller is an important contribution for this paper.*

In order to simplify the equation (4), define

$$\begin{aligned}\varphi_{ij}^q(t)=&2\left[\frac{S_a}{L_a^2}e^{-\frac{\|x_j(t)-x_i(t)-\Delta_{ij}^q\|^2}{L_a^2}}-\frac{S_r}{L_r^2}e^{-\frac{\|x_j(t)-x_i(t)-\Delta_{ij}^q\|^2}{L_r^2}}\right.\\&\left.+\left(\frac{S_r}{L_r^2}+\frac{S_r}{L_a^2}\right)e^{-(\frac{1}{L_r^2}+\frac{1}{L_a^2})(\|x_j(t)-x_i(t)-\Delta_{ij}^q\|^2)}\right].\end{aligned} \tag{6}$$

According to (5), one can verify $\varphi_{ij}^q(t)>0$, and the necessity of this constraint can be addressed by referring that the force vector and position vector are unidirectional.

Then rewrite the formation controller (4) as:

$$u_i^q(t)=\sum_{\substack{j=1\\ j\neq i}}^{N}\varphi_{ij}^q(t)\left(x_j(t)-x_i(t)-\Delta_{ij}^q\right),\quad q\in Q. \tag{7}$$

Remark II.3. *Let $\varphi_{ij}^q(t)$ be a continuous function with respect to $\|x_j(t)-x_i(t)-\Delta_{ij}^q\|$, and it is easy to prove that if the bounds of $\|x_j(t)-x_i(t)-\Delta_{ij}^q\|$ exist, then $\varphi_{ij}^q(t)$ is bounded on all set of $\|x_j(t)-x_i(t)-\Delta_{ij}^q\|$ ($i,j=1,\ldots,N$ and $q\in Q$). Furthermore, regard the fact that most multi-agent systems are implemented in finite horizon which means the limitation of inter-agent distances exists. Throughout the paper, we assume the lower bound of $\varphi_{ij}^q(t)$ exists and denote it as*

$$0<\overline{\varphi}\leq\min_{\substack{i,j=1,\ldots,N\\ q=0,\ldots,m-1}}\varphi_{ij}^q(t), \tag{8}$$

where $\overline{\varphi}>0$ can be guaranteed by choosing appropriate values of L_a,L_r,S_a,S_r in the constraint (5).

III. Analysis of H_∞ formation stability

Now, this section will analyze H_∞ formation stability of the above-developed framework of HMAS in a free and an obstacle-laden environment, respectively.

Since we have property (3), the HMAS (1) is equivalent to

$$\dot{x}_i(t)=f(t,x)+\sum_{j=1}^{N}J_{ij}(t)\left(x_j(t)-x_i(t)\right)+u_i^q(t)+C_iw_i(t). \tag{9}$$

Before moving on, we need to note that the formation switching in the controller will introduce discontinuities to the right hand side of (9). With respect to the dwell-time theory in [27], if the switching of a family of individually stable systems is sufficiently slow, then overall systems remains stable. As a result, we assume that the intervals between consecutive switching signals, i.e. dwell time, are large enough. Due to the introduction of average dwell-time, this assumption does not represent a restriction because this concept allows the formation switching mechanism to be more flexible provided that the average interval between consecutive switching is no less than certain fixed positive constant.

To investigate the formation control of MAS, we introduce a measurement error $X_{ij}(t)$ given as

$$X_{ij}(t)=x_j(t)-x_i(t). \tag{10}$$

It follows from (5), (9) and (10) that the time derivative of $X_{ij}(t)$ is:

$$\begin{aligned}\dot{X}_{ij}(t)=&\sum_{k=1}^{N}\Big(J_{jk}(t)X_{jk}(t)-J_{ik}(t)X_{ik}(t)\Big)\\&+C_jw_j(t)-C_iw_i(t)+\sum_{k=1}^{N}\Big(\varphi_{jk}^q(t)(X_{jk}(t)\\&-\Delta_{jk}^q)-\varphi_{ik}^q(t)(X_{ik}(t)-\Delta_{ik}^q)\Big).\end{aligned} \tag{11}$$

For a formation of multiple agents moving in a clustered environment, it is inevitable to encounter various obstacles which affect the performance of formation, or even break the whole system down. Naturally, the multi-agent system is desirable to be able to adapt to the environment. In general, the agents are only affected by the obstacles when they enter a certain region. At other times, the influence being exerted from obstacles can be negligible. With the above analysis, the obstacles can be treated as exogenous disturbances deriving from the environment, and H_∞ analysis can be employed to investigate the formation stability of HMAS.

Associated the system (2) with the formation controller (7), we define a disagreement function similar to [28]:

$$\Phi(X_{ij}(t)) = \frac{1}{N}\sum_{i=1}^{N-1}\sum_{j>i}^{N}\|X_{ij}(t)-\Delta_{ij}^q\|^2, \tag{12}$$

which demonstrates the formation performance of HMAS for $q \in Q$.

For the HMAS given in (2), H_∞ formation stability means to find a formation controller (7) such that the following conditions in ($\mathbf{DF1}$) and ($\mathbf{DF2}$) hold.

($\mathbf{DF1}$) The formation of HMAS (1) is asymptotically stable when $w(t) = 0$, where $w(t) = [w_1^\top, w_2^\top, \ldots, w_N^\top]^\top$, which is equivalent to the asymptotical formation stability of the HMAS (1) in the absence of obstacles. That is to say, all agents asymptotically converge to the desired formation positions, i.e. $\|X_{ij}(t)-\Delta_{ij}^q\| \to 0$ as $t\to\infty$, where $q\in Q$.

($\mathbf{DF2}$) The formation controller ensures a certain level of H_∞ formation performance as follows:

$$\sup_{\substack{X_{ij}(0)\\ w_i\neq 0}} \frac{\int_0^\infty \Phi(X_{ij}(t))dt}{\frac{1}{4N}\sum\limits_{i=1}^{N}\sum\limits_{j=1}^{N}\|X_{ij}(0)-\Delta_{ij}^q\|^2 + \frac{1}{N}\sum\limits_{i=1}^{N}\|w_i(t)\|_2^2} < \gamma \tag{13}$$

for initial states $x_i(0) \in \mathbb{R}^{n\times 1}$ and $q \in Q$, where $\gamma \geq 1$ is a constant, $X_{ij}(0) = x_j(0) - x_i(0)$ and $\Phi(X_{ij}(t))$ is given by (12). If the conditions ($\mathbf{DF1}$) and ($\mathbf{DF2}$) hold, then the formation of HMAS (1) is said to achieve the H_∞ formation stability.

Remark III.1. *It is worthwhile noting that (*$\mathbf{DF2}$*) is a standard condition arising from the* H_∞ *control theory, which implies that* X_{ij}, $(i,j=1,\ldots,N)$, *converge to* Δ_{ij}^q *in the sense of* $\mathfrak{L}_2$.

Remark III.2. *According to (*$\mathbf{DF2}$*), the attenuation level* $\gamma \geq 1$ *shows the sensitivity of obstacle avoidance in HMAS (1). Giving a smaller* $\gamma \geq 1$ *means the intensity and range of reaction of HMAS towards obstacles are smaller.*

Theorem III.1. *Given a positive scalar* $\gamma \geq 1$*, the* H_∞ *formation problem of the HMAS (1) under the conditions (*$\mathbf{DF1}$*) and (*$\mathbf{DF2}$*) is solved at initial positions* $x_i(0)\in\mathbb{R}^n$ *, if*

$$\begin{bmatrix} -\pi_{ij}+\frac{I}{N} & 0 & 0 & -\frac{C_i}{N}\\ 0 & -\pi_{ij} & \frac{\pi_{ij}+\chi_{ij}}{2} & 0\\ 0 & \frac{\pi_{ij}^\top+\chi_{ij}^\top}{2} & -\chi_{ij} & 0\\ -\frac{C_i^\top}{N} & 0 & 0 & -\frac{2\gamma}{N^2}\end{bmatrix} < 0 \tag{14}$$

holds for all $i,j=1,2,\ldots,N$*, where*

$$\pi_{ij} = \frac{(\overline{\varphi}+J_{ij})\,I}{2},\quad \chi_{ij} = \frac{(\overline{\varphi}-J_{ij})\,I}{2} \tag{15}$$

and $\overline{\varphi}$ *is defined in (8).*

Proof. Without loss of generality, construct a common Lyapunov function in the form of

$$V = \frac{1}{4N}\sum_{i=1}^{N}\sum_{j=1}^{N}\|X_{ij}(t)-\Delta_{ij}^q\|^2, \tag{16}$$

where $q\in Q$. If the derivative of V with respective to (9) is constantly negative for all subsystems, then the formation of HMAS (1) is stable. For the sake of convenience, $X_{ij}(t)$ is implicitly rewritten as X_{ij}, as well as $J_{ij}(t)$, $\varphi_{ij}^q(t)$ and $w_i(t)$ in the proof.

From the above discussion, one has

$$\begin{aligned}\dot V =& \frac{1}{2N}\sum_{i=1}^{N}\sum_{j=1}^{N}\left(X_{ij}-\Delta_{ij}^q\right)^\top \dot X_{ij}\\ =& \underbrace{\frac{1}{2N}\sum_{i=1}^{N}\sum_{j=1}^{N}\sum_{k=1}^{N}\Big[\left(X_{ij}-\Delta_{ij}^q\right)^\top(J_{jk}X_{jk}-J_{ik}X_{ik})\Big]}_{v_1}\\ &\underbrace{+\frac{1}{N}\sum_{i=1}^{N}\sum_{j=1}^{N}\sum_{k=1}^{N}\varphi_{jk}^q\left(X_{ij}-\Delta_{ij}^q\right)^\top\left(X_{jk}-\Delta_{jk}^q\right)}_{v_2}\\ &\underbrace{+\frac{1}{2N}\sum_{i=1}^{N}\sum_{j=1}^{N}\left(X_{ij}-\Delta_{ij}^q\right)^\top(C_jw_j-C_iw_i)}_{v_3}.\end{aligned}$$

In respect that the coupling configuration matrix $J(t)$ is symmetric and $X_{ij}=-X_{ji}$, $\Delta_{ij}^q=-\Delta_{ji}^q$, $X_{ii}=0$ and $\Delta_{jj}^q=0$, one has

$$\begin{aligned}v_1 =& -\frac{1}{N}\sum_{i=1}^{N}\sum_{j=1}^{N}\sum_{k=1}^{N}\left(X_{ji}-\Delta_{ji}^q\right)^\top J_{jk}X_{jk}\\ =& -\frac{1}{N}\sum_{i=1}^{N}\sum_{k=1}^{N}\sum_{k<j}^{N}\left(X_{ji}-\Delta_{ji}^q\right)^\top J_{jk}X_{jk}\\ &\underbrace{-\frac{1}{N}\sum_{i=1}^{N}\sum_{k=1}^{N}\sum_{k>j}^{N}\left(X_{ji}-\Delta_{ji}^q\right)^\top J_{jk}X_{jk}}_{v_{11}}.\end{aligned}$$

Renaming j in the v_{11} as k, thus

$$v_1 = -\frac{1}{N}\sum_{i=1}^{N}\sum_{k=1}^{N}\sum_{k<j}^{N}\Big[\left(X_{ji}-\Delta_{ji}^q\right)^\top-(X_{ki}-\Delta_{ki}^q)^\top\Big]J_{jk}X_{jk}.$$

One can find the fact that $X_{ji}^\top - X_{ki}^\top = X_{jk}^\top$ and $\Delta_{ji}^q-\Delta_{ki}^q=\Delta_{jk}^q$, then

$$\begin{aligned}v_1 =& -\frac{1}{N}\sum_{i=1}^{N}\sum_{k=1}^{N}\sum_{k<j}^{N}\left(X_{jk}-\Delta_{jk}^q\right)^\top J_{jk}X_{jk}\\ =& -\sum_{i=1}^{N}\sum_{j>i}^{N}\left(X_{ij}-\Delta_{ij}^q\right)^\top J_{ij}X_{ij}.\end{aligned} \tag{17}$$

Using the standard completing the square argument, it follows from (17) that

$$\begin{aligned} v_1 =& -\frac{1}{2}\sum_{i=1}^{N-1}\sum_{j>i}^{N} J_{ij}\left\|X_{ij}-\Delta_{ij}^q\right\|^2 \\ & -\frac{1}{2}\sum_{i=1}^{N-1}\sum_{j>i}^{N} J_{ij}\|X_{ij}\|^2 + \frac{1}{2}\sum_{i=1}^{N-1}\sum_{j>i}^{N} J_{ij}\|\Delta_{ij}^q\|^2. \end{aligned} \tag{18}$$

Furthermore, the v_2 is similarly analyzed as follows:

$$v_2 = -\sum_{i=1}^{N}\sum_{j>i}^{N}\varphi_{ij}^q\left(X_{ij}-\Delta_{ij}^q\right)^\top\left(X_{ij}-\Delta_{ij}^q\right).$$

With respect to (8), one can easily obtain

$$\begin{aligned} v_2 \le& -\overline{\varphi}\sum_{i=1}^{N-1}\sum_{j>i}^{N}\left(X_{ij}-\Delta_{ij}^q\right)^\top\left(X_{ij}-\Delta_{ij}^q\right) \\ =&\frac{\overline{\varphi}}{2}\sum_{i=1}^{N-1}\sum_{j>i}^{N}\big(2X_{ij}^\top\Delta_{ij}^q - \|X_{ij}-\Delta_{ij}^q\|^2 \\ & - \|X_{ij}\|^2 - \|\Delta_{ij}^q\|^2\big). \end{aligned} \tag{19}$$

Then, for v_3, one has

$$v_3 = -\frac{2}{N}\sum_{i=1}^{N-1}\sum_{j>i}^{N}\left(X_{ij}-\Delta_{ij}^q\right)^\top C_i w_i. \tag{20}$$

Now, we consider the formation stability of HMAS (1) with $w(t)=0$. From the inequalities (18) and (19), $\dot{V}$ becomes

$$\dot{V} \le \sum_{i=1}^{N-1}\sum_{j>i}^{N}\Omega_{ij}^\top\begin{bmatrix} -\pi_{ij} & 0 & 0 \\ 0 & -\pi_{ij} & \frac{\pi_{ij}+\chi_{ij}}{2} \\ 0 & \frac{\pi_{ij}^\top+\chi_{ij}^\top}{2} & -\chi_{ij}\end{bmatrix}\Omega_{ij},$$

where $\Omega_{ij} = [(X_{ij}-\Delta_{ij}^q)^\top, X_{ij}^\top, (\Delta_{ij}^q)^\top]^\top$, π_{ij} and χ_{ij} are given in (15). By the Schur complement formula, the achievement of inequality (14) is equivalent to the following inequalities satisfied

$$\begin{bmatrix} -\pi_{ij}+\frac{I}{N} & 0 & 0 \\ 0 & -\pi_{ij} & \frac{\pi_{ij}+\chi_{ij}}{2} \\ 0 & \frac{\pi_{ij}^\top+\chi_{ij}^\top}{2} & -\chi_{ij}\end{bmatrix} < 0,$$

and

$$\begin{bmatrix}\frac{C_i}{N} \\ 0 \\ 0\end{bmatrix}^\top \begin{bmatrix} \pi_{ij}-\frac{I}{N} & 0 & 0 \\ 0 & \pi_{ij} & -\frac{\pi_{ij}+\chi_{ij}}{2} \\ 0 & -\frac{\pi_{ij}^\top+\chi_{ij}^\top}{2} & \chi_{ij}\end{bmatrix}^{-1}\begin{bmatrix}\frac{C_i}{N} \\ 0 \\ 0\end{bmatrix} < \frac{2\gamma}{N^2}.$$

By nonnegative matrix theory, one can easily find that

$$\begin{aligned} &\begin{bmatrix} -\pi_{ij} & 0 & 0 \\ 0 & -\pi_{ij} & \frac{\pi_{ij}+\chi_{ij}}{2} \\ 0 & \frac{\pi_{ij}+\chi_{ij}}{2} & -\chi_{ij}\end{bmatrix} \\ \le& \begin{bmatrix} -\pi_{ij}+\frac{I}{N} & 0 & 0 \\ 0 & -\pi_{ij} & \frac{\pi_{ij}+\chi_{ij}}{2} \\ 0 & \frac{\pi_{ij}^\top+\chi_{ij}^\top}{2} & -\chi_{ij}\end{bmatrix} < 0, \end{aligned} \tag{21}$$

which implies $\dot{V}<0$. This proves that condition ($\mathbf{DF1}$) holds for the HMAS (1) with $w(t)=0$.

Next, we prove the H_∞ performance constraint ($\mathbf{DF2}$) for all nonzero $w_i(t)\in\mathfrak{L}_2[0,\infty)$ and a prescribed $\gamma\ge 1$. Define

$$\begin{aligned} \widetilde{V} =& \int_0^\infty\left(\Phi(X_{ij}(t)) - \gamma\frac{1}{N}\sum_{i=1}^{N} w_i^\top(t)w_i(t)\right)dt \\ & - \frac{\gamma}{2N}\sum_{i=1}^{N-1}\sum_{j>i}^{N}\|x_j(0)-x_i(0)-\Delta_{ij}^q\|^2, \end{aligned}$$

and one has

$$\begin{aligned} \widetilde{V} =& \int_0^\infty\Big(\Phi(X_{ij}(t)) - \frac{\gamma}{N}\sum_{i=1}^{N} w_i^\top(t)w_i(t) + \dot{V}\left(x(t)\right)\Big)dt \\ & - V\left(x(\infty)\right) + \frac{1-\gamma}{2N}\sum_{i=1}^{N-1}\sum_{j>i}^{N}\|x_j(0)-x_i(0)-\Delta_{ij}^q\|^2 \\ \le& \int_0^\infty\underbrace{\left(\Phi(X_{ij}(t)) - \frac{\gamma}{N}\sum_{i=1}^{N}\|w_i(t)\|^2 + \dot{V}\left(x(t)\right)\right)}_{\Xi}dt. \end{aligned} \tag{22}$$

Combining (18), (19) and (20) one obtains

$$\begin{aligned} \Xi =& \sum_{i=1}^{N}\sum_{j=1}^{N}\Bigg\{\frac{1}{2N}\|X_{ij}-\Delta_{ij}^q\|^2 - \frac{\gamma}{N^2}w_i^\top w_i \\ & - \frac{1}{N}\left(X_{ij}-\Delta_{ij}^q\right)^\top C_i w_i \\ & + \Omega_{ij}^\top\begin{bmatrix} -\frac{\pi_{ij}}{2} & 0 & 0 \\ 0 & -\frac{\pi_{ij}}{2} & \frac{\pi_{ij}+\chi_{ij}}{4} \\ 0 & \frac{\pi_{ij}^\top+\chi_{ij}^\top}{4} & -\frac{\chi_{ij}}{2}\end{bmatrix}\Omega_{ij}\Bigg\} \\ =& \sum_{i=1}^{N}\sum_{j=1}^{N}\xi_{ij}^\top\begin{bmatrix} -\frac{\pi_{ij}}{2}+\frac{I}{2N} & 0 & 0 & -\frac{C_i}{2N} \\ 0 & -\frac{\pi_{ij}}{2} & \frac{\pi_{ij}+\chi_{ij}}{4} & 0 \\ 0 & \frac{\pi_{ij}^\top+\chi_{ij}^\top}{4} & -\frac{\chi_{ij}}{2} & 0 \\ -\frac{C_i^\top}{2N} & 0 & 0 & -\frac{\gamma}{N^2}\end{bmatrix}\xi_{ij}, \end{aligned}$$

where $\xi_{ij} = [\Omega_{ij}^\top, w_i^\top(t)]^\top$. From the LMI (14), it is easy to prove $\Xi<0$ which implies $\widetilde{V}<0$ and immediately leads to the inequality (13).

Therefore, the formation of HMAS (1) has the property of H_∞ criteria ($\mathbf{DF1}$) and ($\mathbf{DF2}$). This completes the proof. □

Remark III.3. *By studying the LMIs* (14), *the variables* $\chi_{ij} > 0$ *in* (15) *indicate the connectivity strength among agents. In particular, due to the monotone decreasing property of* φ_{ij} *with respect to norm* $\|x_j(t)-x_i(t)-\triangle_{ij}\|$ *and the discussion in* ***Remark*** *II.3, this connectivity strength is inversely proportional to the relatively active scope of MASs.*

IV. Design Obstacle-avoiding Functions

In this section, collision avoidance in trajectory tracking is achieved using mutual repulsion between agents and obstacles, which is resulted from the Newtonian potential-based model. By regarding the agents and obstacles as conductors with uniform charges, the repulsive force in inversely proportional to the distance of them, can be derived in closed form.

Based on practical applications in robotics and haptic rendering, an ideal potential field should possess all of the following attributes.

(i) With respect to the property of obstacle avoidance, the magnitude of potential and corresponding repulsion should be infinite at the boundary of obstacles and drop off with distance. And the range of potential is bounded, which is accordant with the limited detective scope of agent's built-in explorer in this paper.

(ii) The shapes of equipotential surface should be similar with the obstacle surface, and spherical symmetrical at the boundary of potential field.

(iii) The first and second derivatives of potential function should exist and be continuous, so that the resulting force field is smooth.

Before moving on, for making this paper self-contained, we revisit the general definition of external disturbance in the H_∞ problem. H_∞ techniques are usually used to evaluate the incremental gain of external input signal in any direction and at any frequency. In the context of H_∞ theory, the external signals with finite energy are often investigated, i.e. $\|w(t)\| \leq \infty$. More explicitly, the finite energy signal $w(t)$ is said to belong to $L_2[0,\infty)$, which implies

$$\left[\int_0^\infty \|w(t)\|^2 dt\right]^{1/2} = \left[\int_0^\infty \sum_{i=1}^N w_i^\top(t) w_i(t) dt\right]^{1/2} < \infty.$$

In order to utilize H_∞ theory to design obstacle-avoidance controller, we assume that multi-agent systems ultimately get far from the obstacles as time evolves. Incorporated with attributes (ii) this assumption leads to $\lim_{t\to\infty} w(t) = 0$. That is, the obstacle-avoidance functions $w_i(t)$ are available in finite time intervals. In addition, for avoiding obstacles, the agent-obstacle distances are intuitively greater than zero, and consequently the supremum of function $w_i(t)$ $(i = 1, \ldots, N)$ is existed. Based on above analysis on obstacle-avoidance function, one can easily derive the conclusion that $w(t)$ belongs to $L_2[0,\infty)$.

Now, we will discuss the obstacle-avoiding function beginning with the instance of mass points (when the bulks of agents and obstacles are close to each other), and then extend to bulky obstacles (over 10 times bigger than agent) with arbitrary shapes.

Consider an agent i navigates in an obstacle-laden environment with $M \in \overline{\mathbb{Z}}_+$ obstacles, and assume $s_l \in \mathbb{R}^n$ is the position of obstacle l $(l \in \{1, 2, \ldots, M\})$. The potential at agent i due to obstacle l is

$$P_{il}^o(t) = \frac{\rho_{il}}{\|x_i(t) - s_l\|}, \tag{23}$$

where ρ_{il} is the repulsion coefficient for obstacles avoidance and defined as follows:

$$\rho_{il} = \begin{cases} \rho, & \|x_i(t) - s_l\| < \delta \\ 0, & \|x_i(t) - s_l\| \geq \delta, \end{cases} \tag{24}$$

where ρ is a positive scalar and δ is the maximal sensing range of agent. When the relative distance of agent i and obstacle l is shorter than the detective scope δ, agent i will receive a signal of possible collision and the obstacle-avoiding function will work. In other words, the repulsive potentials between agents and obstacles act only when they get close to certain range. Now, the obstacle-avoiding function for agent i is introduced based on the negative gradient of the potential (23) in the following form

$$w_i(t) = -\nabla_{x_i} P_{il}^o(x_i, s_l) = \sum_{l=1}^M \rho_{il} \frac{x_i(t) - s_l}{\|x_i(t) - s_l\|^3}. \tag{25}$$

Then we extend the obstacle-avoiding function for bulky objects with arbitrary shapes. In practical situations, particularly in many exploration applications, the implicit functions of obstacles to be modeled are not available. But by samples of boundary surfaces obtained from camera, laser range finder and sonar and with the help of some techniques such as signal sampling and image processing, the implicit functions can be obtained and then to construct the APFs [20]. For convenience, in this paper, assume the boundary function of obstac le l is known as $\mathbf{B}_l$, and β_l here is the position of arbitrary point on the boundary of obstacle. In fact, most of obstacles can be mathematically approximate with polyhedron. In this paper we focus on the convex polyhedra obstacles. Moreover, the results can be easily extended to obstacles with arbitrary shapes. The repulsion between agent i and an arbitrary point of the obstacle's boundary is

$$F_{il}^o(t) = \rho_{il} \frac{x_i(t) - \beta_l}{\|x_i(t) - \beta_l\|^3},$$

where ρ_{il} are defined in (24). Then for the agent i the obstacle-avoiding function is defined as

$$w_i(t) = \sum_{l=1}^M \oint_{B_l} dF_{il}^o, \tag{26}$$

where $\oint_{B_l}$ represents the surface integrals on boundary of obstacles.

In view of above analysis, the obstacles laden in the terrain are static. However, it is worth mentioning that all the obstacle-avoidance functions are available for moving obstacles except for those with high-speed. In this case, the position vector $\beta_l(t)$ is a vector-valued function over time $t \in \mathbb{J}$.

V. Numerical Examples

In this section some simulation results illustrate the performance of the proposed control laws to achieve formation and obstacles avoidance. To avoid triviality, the advantage of formation controllers (4) compared with others is omitted in this paper and the reader is referred to [1].

Firstly, drive 4 agents with the initialization positions $(-1.2, -1.1)^\top$, $(-2.0, 3.8)^\top$, $(5.3, 2.0)^\top$ and $(4.2, 2.0)^\top$, to form a shape of square and realize obstacle avoidance in the navigation. The formation-shape matrix Δ^q is set as

$$\Delta_{12}^1 = [\frac{\sqrt{2}}{2}, \frac{\sqrt{2}}{2}]^\top, \qquad \Delta_{23}^1 = [\frac{\sqrt{2}}{2}, -\frac{\sqrt{2}}{2}]^\top,$$
$$\Delta_{34}^1 = [-\frac{\sqrt{2}}{2}, -\frac{\sqrt{2}}{2}]^\top, \qquad \Delta_{41}^1 = [-\frac{\sqrt{2}}{2}, \frac{\sqrt{2}}{2}]^\top,$$
$$\Delta_{13}^1 = [\sqrt{2}, 0]^\top, \qquad \Delta_{24}^1 = [0, -\sqrt{2}]^\top$$

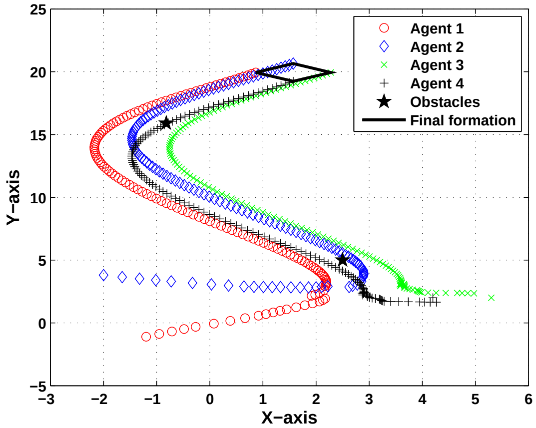

Fig. 2. Formation of MAS without obstacle-avoidance functions case

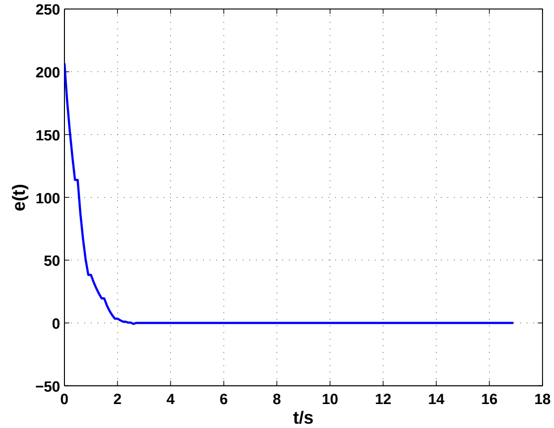

Fig. 4. Formation error of MAS controlled by obstacle-avoidance functions

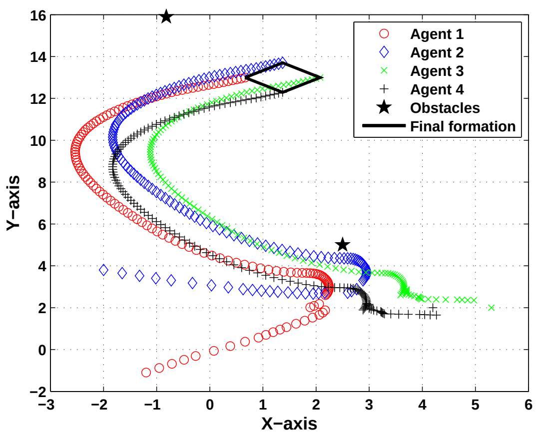

Fig. 3. Formation of MAS with obstacle-avoidance functions case

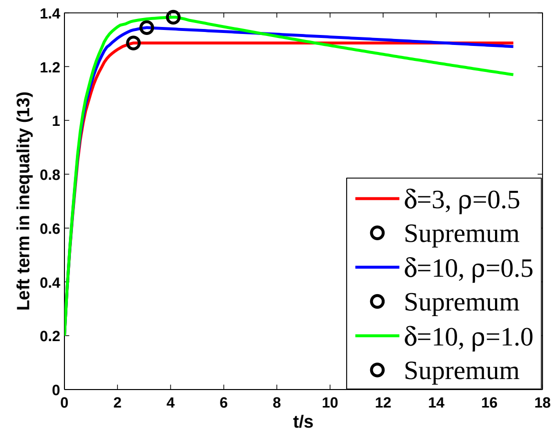

Fig. 5. Investigation of parameter γ, ρ, δ

and two obstacles locate at $[2.50, 5.00]^\top$ and $[-0.82, 15.90]^\top$. The target trajectory of $f(t, x)$ in HMAS (1) is given by

$$f(t, x) = \begin{bmatrix} -0.1 & 0 \\ 0 & 0.1 \end{bmatrix} x_i + \begin{bmatrix} \cos(0.4 * t) \\ \sin(0.25 * t) \end{bmatrix}$$

and the time-varying configuration matrix switches from one mode to another. They are:

$$J^1 = \begin{bmatrix} -0.6 & 0.3 & 0 & 0.3 \\ 0.3 & -0.6 & 0.3 & 0 \\ 0 & 0.3 & -0.6 & 0.3 \\ 0.3 & 0 & 0.3 & -0.6 \end{bmatrix}$$

and

$$J^2 = \begin{bmatrix} -0.9 & 0.3 & 0.3 & 0.3 \\ 0.3 & -0.9 & 0.3 & 0.3 \\ 0.3 & 0.3 & -0.9 & 0.3 \\ 0.3 & 0.3 & 0.3 & -0.9 \end{bmatrix}.$$

For the formation controller (5), let $S_a = 8.1$, $L_a = 0.31$, $S_r = 0.69$, $L_R = 0.3$, and $\delta = 3$, $\rho = 0.5$ in obstacle-avoiding function (25).

According to Fig. 2 and Fig. 3 one can demonstrate the control laws presented in this paper realize the formation keeping while avoiding collision with obstacles (marked by black stars in the figures) in complex environment. For the sake of measuring and visualising the formation effectiveness, we introduce the following formation error

$$e(t) = \sum_{i=1}^{N-1} \sum_{j>i}^{N} (\|x_j(t) - x_i(t)\| - \|\Delta_{ij}^q\|),$$

which is shown in Fig. 4. Then, the sensitivity of obstacle-avoiding function is investigated in Fig. 5, which depicts the curves of left term in inequality (13) under different repulsion coefficient ρ and repulsion rang δ. From Fig. 5, one can verify the fact that the performance index γ in inequality (13) reflects the sensitivity of HMAS towards obstacles, i.e. smaller γ requires HMAS less active (smaller ρ and δ) towards obstacle.

Next, in an attempt to demonstrate the effectiveness of obstacle-avoidance function (26), a rectangle obstacle stands in the way of the HMAS path. Fig. 6 and Fig. 7 show the HMAS steers around the obstacle smoothly with the help of obstacle-avoidance functions and keeps a predefined formation in the whole process, as well as the corresponding formation

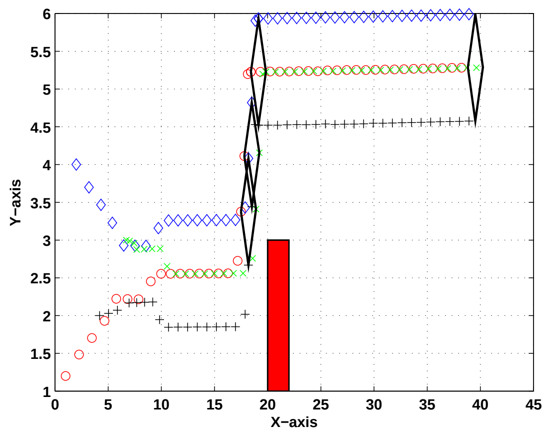

Fig. 6. Obstacle avoidance of MAS in 2-D

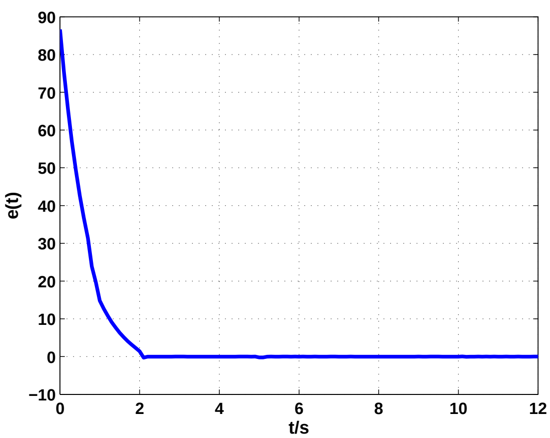

Fig. 7. Formation error for obstacle avoidance of MAS in 2-D

error.

In many practical situations, the HMAS occasionally encounters the trench-shape obstacles which are impossible for the whole system keeping original shape to pass through. In such case, the HMAS has to transform formation to a feasible one. In this example, task is to transition from a square formation to a straight line to pass the trench safely. When the HMAS detects the trench existed in the tracking path, specified task is triggered and corresponding formation is determined according to the predetermined task-formation scheme. As shown in Fig. 8, the HMAS breaks formation and go in a straight line when meets the trench and transforms back into the original formation after passing the trench.

VI. Conclusion

In this article, new formation and obstacle-avoidance protocols of multi-agent systems are presented. A notion of H_∞ formation has been first defined to characterize the performance of obstacle-avoiding, and the H_∞ performance index is concreted as a sensitivity of obstacle-avoidance in this paper. Then a hybrid formation controller with a task set and a formation set is introduced to handle distinct obstacles. By

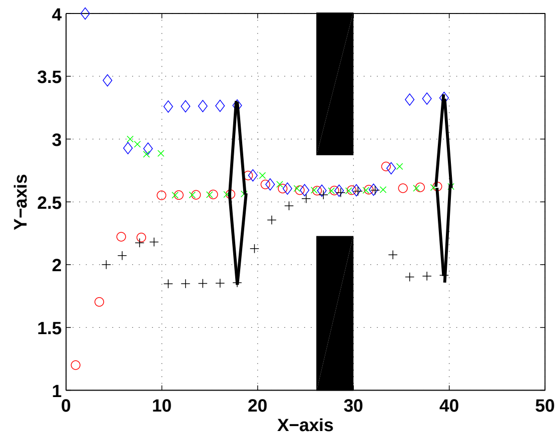

Fig. 8. Formation change for HMAS in the presence of trench-shaped obstacle

designing diverse task-formation mapping, the HMAS can accomplish various complex missions. Then obstacle-avoidance functions using potential field model are specified to realize multi-agent systems avoiding arbitrarily shaped obstacles on the path. According to the simulation results, not only can the HMAS steer around the obstacles with proposed approach, but the reconfiguration of formation can be achieved in the complex environment.

A. *Acknowledgements*

This work was supported by the National Natural Science Foundation of China under Grants 61174158, 61034004 and 61272271, Special Financial Grant from the China Postdoctoral Science Foundation (No.201104286), China Postdoctoral Science Foundation funded project 2012M510117, Natural Science Foundation Program of Shanghai (No.12ZR1434000) and the Fundamental Research Funds for the Central Universities.

References

[1] D. Xue, J. Yao, G. Chen, and Y. Yu, "Formation control of networked multi-agent systems," *IET Control Theory and Application*, vol. 4, pp. 2168–2176, 2010.

[2] J. Desai, J. Ostrowski, and V. Kumar, "Modeling and control of formations of nonholonomic mobile robots," *IEEE Transactions on Robotics and Automation*, vol. 17, pp. 905–908, 2001.

[3] S. Critaldi, A. Ferro, R. Giugno, G. Pigola, and A. Pulvirenti, "Obstacles constrained group mobility models in event-driven wireless networks with movable base stations," *Ad Hoc Network*, vol. 9, pp. 400–417, 2011.

[4] X. Wang, V. Yadav, and S. Balakrishnan, "Cooperative uav formation with obstacle/collision avoidance," *IEEE Transactions on Control Systems Tehcnology*, vol. 4, pp. 672–679, 2007.

[5] Q. Hui, "Finite-time rendezvous algorithms for mobile autonomous agents," *IEEE Transactions on Automatic Control*, vol. 56, pp. 207–211, 2011.

[6] R. Olfati-Saber, "Flocking for multi-agent dynamic systems: Algorithms and theory," *IEEE Transactions on Automatic Control*, vol. 51, pp. 401–420, 2006.

[7] V. Gazi and K. Passino, "Stability analysis of social foraging swarms," *IEEE Transations on Systems, Man, and Cybernetics - Part B: Cybernetics*, vol. 34, pp. 539–555, 2004.

[8] F. Zhang, "Geometric cooperative control of particle formations," *IEEE Transactions on Automatic Control*, vol. 55, pp. 800–804, 2010.

[9] M. Defoort, T. Floquet, A. K$\ddot{o}$k$\ddot{o}$sy, and W. Perruquetti, "Sliding-mode formation control for cooperative autonomous mobile robots," *IEEE Transactions on Industrial Electronics*, vol. 55, pp. 3944–3953, 2008.

[10] T. Kim and T. Sugie, "Cooperative control for target-capturing task based on a cyclic pursuit strategy," *Automatica*, vol. 43, pp. 1426–1431, 2007.

[11] S. Ge and C. Fua, "Queues and artificial potential trenches for multirobot formations," *IEEE Transactions on Robotics*, vol. 21, pp. 646–656, 2005.

[12] R. Olfati-Saber and R. Murray, "Graph rigidity and distributed formation stability of multi-vehicle systems," pp. 2965–2971, 41st IEEE Conference on Decision and Control, 2002.

[13] M. Karasalo and X. Hu, "Robust formation control and servoing using switching range sensors," *Robotics and Autonomous Systems*, vol. 58, pp. 1003–1016, 2010.

[14] B. Shen, Z. Wang, and X. Liu, "Bounded h_∞ synchronization and state estimation for discrete time-varying stochastic complex networks over a finite horizon," *IEEE Transactions on Neural Networks*, vol. 22, pp. 145–5–157, 2011.

[15] J. Guerrero, G. Romero, and R. Lozano, "Robust consensus tracking of leader-based multi-agent systems," pp. 6299–6305, American Control Conference, Jun. 2010.

[16] V. Gazi, "Swarm aggregations using artificial potentials and sliding-mode control," *IEEE Transations on Robotics*, vol. 21, pp. 1208–1214, 2005.

[17] O. Khatib, "Real time obstacle avoidance for manipulators and mobile robots," *International Journal of Robotics Researches*, vol. 5, pp. 90–98, 1986.

[18] D. Bennet and C. McInnes, "Distributed control of multi-robot systems using bifurcating potential fields," *Robotics and Autonomous Systems*, vol. 58, pp. 256–264, 2010.

[19] J. Chuang and N. Ahuja, "An analytically tractable potential field model of free space and its application in obstacle avoidance," *IEEE Transactions on Systes, Man, and Cybernetics - Part B: Cybernetics*, vol. 28, pp. 729–736, 1998.

[20] J. Ren, K. McIsaac, R. Patel, and T. Peters, "A potential field model using generalized sigmoid functions," *IEEE Transactions on Systems, Man, and Cybernetics - Part B: Cybernetics*, vol. 37, pp. 477–484, 2007.

[21] A. Eresen, N. $\dot{I}$mamo$\tilde{g}$lu, and M. $\ddot{O}$nder Efe, "Autonomous quadrotor flight with vision-based obstacle avoidance in virtual environment," *Expert Systems with Applications*, vol. 39, pp. 894–905, 2012.

[22] D. Parhi and J. Mohanta, "Navigational control of several mobile robotic agents using petri-potential-fuzzy hybrid controller," *Applied Soft Computing*, vol. 11, pp. 3546–3557, 2011.

[23] M. Heymann, F. Lin, and G. Meyer, "Control synthesis for a class of hybrid systems subject to configuration based on safety constraints," *NASA Technical Memorandum 112196*, 1997.

[24] M. Heymann, F. Lin, and G. Meyer, "Synthesis and viability of minimally interventive legal controllers for hybrid systems," *Discrete Event Dynamic System: Theory and Application*, vol. 8, p. 105135, 1998.

[25] J. Yao, F. Lin, and B. Liu, "h_∞ control for stochastic stability and disturbance attenuation in a class of networked hybrid systems," *IET Control Theory and Application*, vol. 5, pp. 1–11, 2011.

[26] C. Cassandras and S. Lafortune, *Introduction to Discrete Event System*. Springer, 2008.

[27] R. Shorten, F. Wirth, O. Mason, and K. Wulff, "Stability criteria for swtiched and hybrid systems," *SIAM Review*, vol. 49, pp. 545–592, 2005.

[28] R. Olfati-Saber and R. Murray, "Consensus problems in networks of agents with switching topology and time-delays," *IEEE Transactions on Automatic Control*, vol. 49, pp. 1520–1533, 2004.